J Mater Sci (2007) 42:6274–6278
DOI 10.1007/s10853-006-1249-3

Study of electrical conductivity changes and phase transitions in TiO_2 doped ZrO_2

Saba Beg · Pooja Varshney · Sarita

Received: 25 May 2006 / Accepted: 10 November 2006 / Published online: 21 April 2007

Abstract The electrical conductivity in ZrO_2 doped with various molar ratios of TiO_2 has been measured at different temperatures. Phase transitions depending on the temperature for different molar compositions were investigated by doping of the samples. The conductivity is also found to increase with rise in temperature till 200 °C and thereafter decreases due to collapse of the fluorite framework. A second rise in conductivity in the doped samples around 462 °C is observed due to phase transition of ZrO_2. X-ray powder diffraction recorded at high temperature show the effect of doping and the phase relationships of doped materials. DTA was also carried out for confirming doping effect and phase transition in samples.

Introduction

Many studies have been done, experimental as well as theoretical, on the electronic and structural properties of titanium dioxide. Titanium dioxide is known to occur in two phases: rutile and anatase. However, only the rutile phase has been studied extensively. Rutile is an important rock-forming mineral and the most abundant titanium dioxide polymorph in nature. In addition, most crystal-growth techniques basically yield titanium dioxide in the rutile phase. Anatase is less dense than rutile and is also found to be less stable [1, 2]. It is well known, that titanium dioxide appears as high-pressure phases that are isostructural with columbite (orthorhombic a-PbO_2) and baddeleyite (monoclinic ZrO_2) [1, 3, 4].

Zirconia-based ceramics have numerous applications. While pure zirconia (ZrO_2) is used as a refractory material, when doped with aliovalent ions it has structural applications. In particular, to produce a ceramic that is both strong and tough, doping can control the monoclinic-to-tetragonal transition. Moreover, doping with lower valent cations introduces oxygen vacancies whose high mobility leads to high ionic conductivity that is exploited in, for example, solid electrolytes for high-temperature fuel cells and in gas sensors [5]. The high oxygen vacancy concentration gives rise to high oxygen-ion mobility. Oxygen-ion conduction takes place in stabilized ZrO_2 by movement of oxygen ions via vacancies. Over a wide range of temperature, the ionic conductivity of stabilized ZrO_2 is independent of oxygen partial pressure over several orders of magnitude [6].

TiO_2–ZrO_2 system has been used in a wide range of applications, such as electronic industry (useful dielectric properties in the microwave frequency regime), high-temperature pigments, technical and structural ceramics [7–17]. Wang et al. [18] have reported that the composition of TiO_2–ZrO_2 affects the resultant surface area and activity. It should be noted that in a previous research, Daly et al. concluded that the preparation methodology for TiO_2–ZrO_2 not only affects its physical properties, such as surface area and porosity, but also its surface chemistry [19].

This work was carried out in order to investigate the effect of TiO_2 doping in ZrO_2. The effects of temperature and doping ratio, on electrical conductivity of ZrO_2 were investigated. X-ray powder diffraction and DTA were done to study the effect of doping and the phase relationships of materials.

S. Beg (✉) · P. Varshney · Sarita
Department of Chemistry,
Aligarh Muslim University, Aligarh 202002, India
e-mail: beg_saba@yahoo.co.in

Experimental

ZrO_2 (Aldrich, 99.99 % pure) was doped with 2, 4, 6 and 8 mol% of TiO_2 (Merck, 98% pure). The materials in the above ratios were mixed and grinded in an agate mortar and then pressed at a pressure level of 490 MPa with the help of hydraulic press (Spectralab Model SL-89) to prepare the samples in the form of pellets having diameter of 2.4 cm and thickness 0.1 cm. These pellets were then annealed at 1,000 °C for 28 h in a muffle furnace.

The a.c. conductivity measurements were carried out by the two-probe method in the temperature range 30–900 °C using a GENRAD 1659RLC Digibridge at different frequencies (10 kHz, 1 kHz, 120Hz and 100Hz). The rate of heating was maintained at 1 °C/min.

Thermal analysis of the various molar compositions was performed by using DTA/TG system (Shimadzu DT-40 type) and heating rate was 20 °C per minute.

Powder diffraction data of the samples were recorded with XTRA 50 made by Thermo Electroon 2 Diffractometer with monochromator CuKα radiation operated at 40 kV and 40 mA. Diffraction patterns were scanned by steps 0.002° (2θ) over the angle rang 20–80° (2θ).

Results and discussion

Conductivity studies

The temperature dependence of the ionic conductivity is expressed by the Arrhenius equation:

$$\sigma = ne^2\lambda^2 \nu y/kT \exp(-\Delta G^*/kT) \quad (1)$$

$$= ne^2\lambda^2 \nu y/kT \exp(\Delta S^*/k - \Delta H^*/kT), \quad (2)$$

where n is the number of ions per unit volume, e the ionic charge, λ the distance between two jump positions, ν the jump frequency, y the intersite geometry constant and ΔG^*, ΔS^* and ΔH^* are activation free energy, entropy and enthalpy terms respectively. The equation can be written in a simpler form as,

$$\sigma T = \sigma_0 \exp(-E_a/kT), \quad (3)$$

σ_0 being equal to $ne^2\lambda^2\nu y/k\exp(\Delta S^*/k)$ and $\Delta H^* = E_a$, the activation enthalpy equals the experimental activation energy for ionic motion [20].

Figure 1 shows the rise in isothermal conductivity as the level of substitution increases, at room temperature. In general zirconia-based materials, lower valent cations (Ca^{2+}, Y^{3+}) enhance the ionic conductivity by substituting

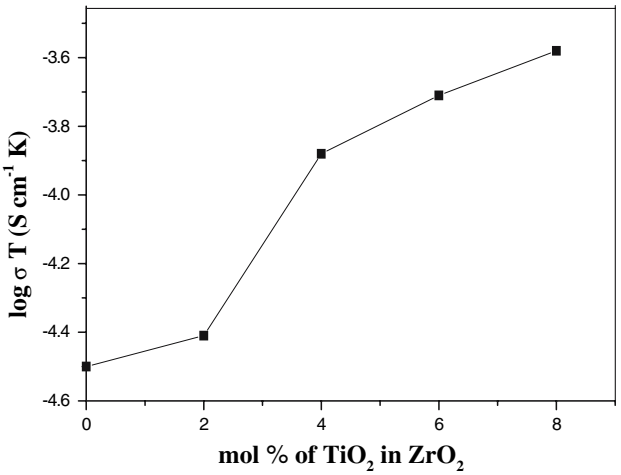

Fig. 1 Compositional variation of room temperature conductivity of TiO_2 in ZrO_2

normal zirconium sites and creating additional ionic charge carriers (in this case, oxygen vacancy) to maintain charge neutrality. Creation of the additional oxygen vacancies over intrinsic anionic Frenkel defects is a very important factor for the application of zirconia as a solid electrolyte [21]. The stabilization process of TiO_2–ZrO_2 system is quite different from that of general cases of addition of aliovalent cations. In this case Ti^{4+} ion occupying a zirconium site cannot introduce any additional oxygen vacancy, as zirconium ion and titanium ion are isovalent.

Nevertheless, it is known that the oxygen vacancy formation can also be encouraged by the strain energy induced by the size difference between dopant and host cations, and thus the enhancement of the ionic conductivity can be observed even in the case of isovalent doping [21–24]. The size of Ti^{4+} (0.68 Å) is lesser than Zr^{4+} (0.79 Å) and consequently this size difference could encourage the creation of oxygen vacancies. This phenomenon is often called as ''size effect'' [21, 25]. It is normally recognized that the size difference between dopant and host ions causes the distortion of lattice structure and lowers the activation energy of oxygen vacancy formation [25].

We therefore conclude, that the rise in conductivity with increase in concentration of TiO_2 is due to migration of oxygen vacancies, created as a result of 'size effect'.

The variation in conductivity measured at 10 kHz, with temperature for TiO_2–ZrO_2 system is shown in Fig. 2. It may be seen that the conductivity variations for the various compositions follow a uniform pattern. As is evident from Fig. 2, conductivity of all the compositions initially increases with rise in temperature till 200 °C and then decreases. The initial increase in conductivity with rise in temperature is due to increase in rate of migration of vacancies and interstitial oxygen ions [26]. Interstitial oxygen ions are partly responsible for ionic conduction in

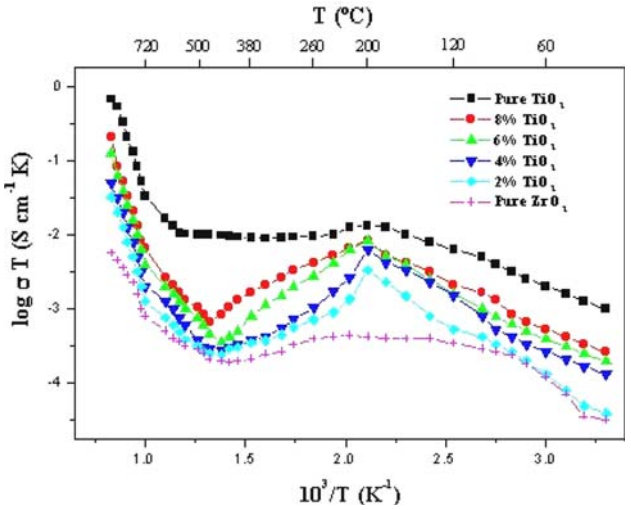

Fig. 2 The temperature dependence of electrical conductivity for TiO_2–ZrO_2 system

samples. A marked drop in conductivity above 200 °C was considered to be due to collapse of the fluorite framework, since on cooling, the higher conductivity is regained and no hysteresis is observed (Fig. 3). This supported the argument of lattice collapse, and its subsequent recovery on cooling, employing restructuring of the sublattice. Such type of decrease in conductivity has been reported earlier [27–29].

A rise in conductivity from about 460 °C takes place for pure ZrO_2, as its phase transition from monoclinic to tetragonal starts around 460–500 °C, and is completed around 1,160 °C [30, 31]. All the doped samples also show a second rise in conductivity due to this phase transition of ZrO_2, in the temperature range 460–500 °C. It was

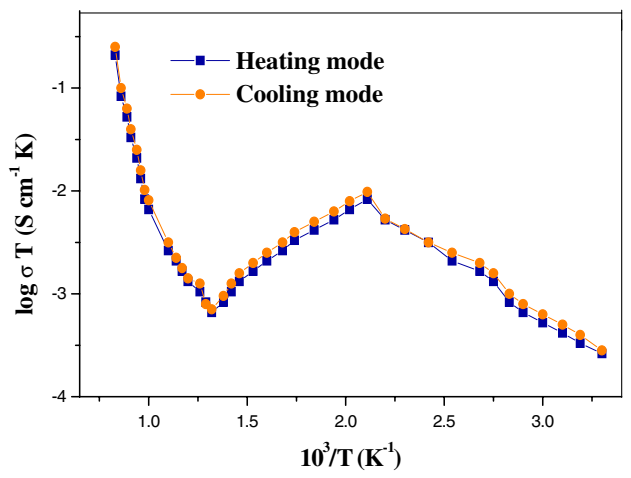

Fig. 3 The temperature dependence of electrical conductivity of TiO_2 -doped-ZrO_2 in heating and cooling mode higher dopant content (8% TiO_2)

observed, that this rise in conductivity shifts to higher temperatures as the percentage of TiO_2 increases.

Conductivity variation with temperature for all the samples has also been studied at 1 kHz, 120Hz and 100Hz as well, and it was found that the change in frequency does not induce any change in the electrical conductivity behavior.

The activation energy E_a for various molar ratios, has been calculated in the temperature ranges 500–700 and 720–900 °C, and shown in Table 1. As seen in the Table, activation energy value is almost constant. It may confirm the correlation of the constant values in E_a, which is a function of the electronic energy levels of the chemically interacting atoms. Constancy of E_a implies that crystallographic surroundings of the constituents of conduction, that are oxygen ions and vacancies, do not exhibit any appreciable change with increasing doping. Higher doping introduces more defects into the structure [32].

Differential thermal analysis

The results of DTA are shown in Fig. 4. For pure ZrO_2, the DTA curve shows an exothermic peak at 460 °C due to the phase transition of ZrO_2 from monoclinic to tetragonal. As is evident from the figure, on doping ZrO_2 with TiO_2 the exothermic peak shifts to higher temperatures. We therefore conclude that the phase transition of ZrO_2 shifts to higher temperatures on doping. These results are in good agreement with the conductivity results described earlier.

X-ray powder diffraction

The X-ray diffractogram for 4 and 8-mol% TiO_2 recorded 800, 900 and 1,000 °C, and are shown in Fig. 5a and b respectively. In the diffractograms recorded at 800 °C, for 4-mol% TiO_2 (Fig. 5a) and 8-mol% TiO_2 (Fig. 5b), large diffraction peaks, indicated by *M*, are attributed to the monoclinic phase of ZrO_2 (reflections at 28.6° and 31.8°) and one small diffraction peak is observed for tetragonal phase of ZrO_2 indicated by *T* (reflection at 30.3°). However, when the diffractograms for the same samples were

Table 1 Activation energies for various molar ratios at different temperature ranges

Sample composition (mol% of TiO_2)	Activation energy (ev)	
	E_{a1} (500–700 °C)	E_{a2} (720–900 °C)
2	0.54	1.63
4	0.56	1.63
6	0.56	1.75
8	0.61	1.75

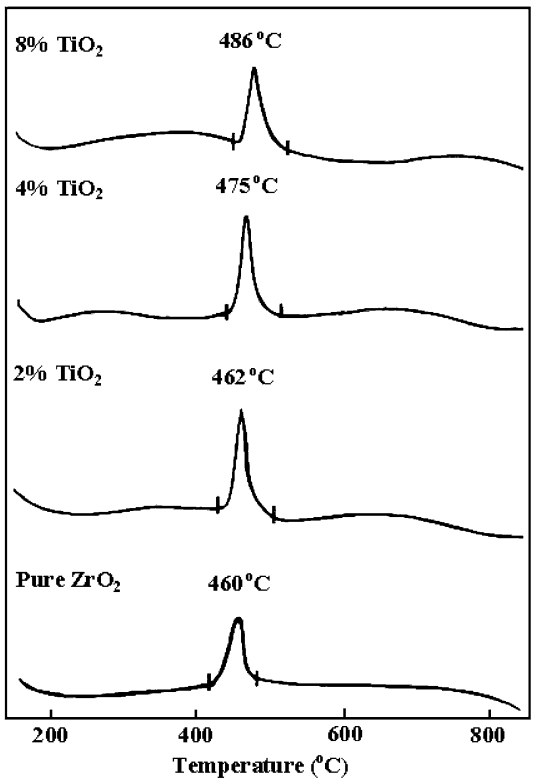

Fig. 4 DTA curves for TiO_2–ZrO_2 system

recorded at 900 and 1,000 °C, more intense peak for tetragonal phase of ZrO_2 was obtained along with the peaks for monoclinic phase of ZrO_2. This is due to the fact, that upon increasing the concentration of dopant, the tetragonal ZrO_2 gradually increases. Higher temperature phases are said to be retained at lower temperatures by doping [33–35]. It may therefore be concluded that the phase composition is influenced by the presence of dopant [36].

Conclusion

The electrical conductivity of ZrO_2 is found to be enhanced markedly in the temperature range 120–300 °C, on doping with TiO_2. Initially the conductivity increases with temperature due to increase in rate of migration of vacancies and interstitial oxygen ions, and then decreases beyond 220 °C due to collapse of the fluorite framework. A second rise in conductivity and an exothermic peak in DTA at 460 °C confirm the phase transition in pure ZrO_2 from monoclinic to tetragonal but in the doped samples this transition shifts to higher temperatures.

Acknowledgements The authors are grateful to Dr. Steven L. Suib (USA) for providing X-ray measurements. The authors are also thankful to UGC New Delhi (F.30–83/2004) for financial assistance.

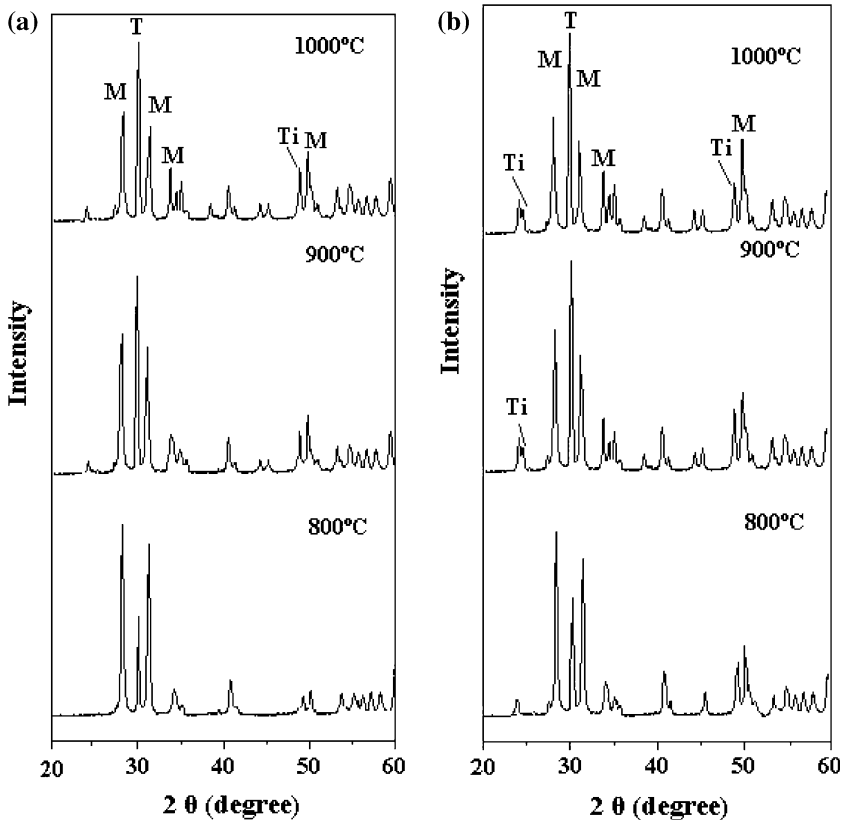

Fig. 5 (**a**) X-ray diffraction patterns for 4-mol% TiO_2 at different temperatures. (**b**) X-ray diffraction patterns for 8-mol% TiO_2 at different temperatures

References

1. Arlt T, Bermejo M, Blanco MA, Gerward L, Jiang JZ, Olsen JS, Recio JM (2000) Phys Rev B 61:14 414
2. Fahmiand A, Minot C (1993) Phys Rev B 47:17717
3. Gou B, Liu Z, Cui Q, Yang H, Zhao Y, Zou G (1989) High Press Res 1:185
4. Liu LG, Mernagh TP (1992) Eur J Mineral 4:45
5. Schelling PK, Phillpot SR, Wolf D (2001) J Am Ceram Soc 84:1609
6. Minh NQ (1993) J Am Ceram Soc 76:563
7. Wolfram G, Gobel E (1981) Mater Res Bull 16:1455
8. Swatrz SL, Shrout TR (1982) Mater Res Bull 17:1245
9. Mchale AE, Roth RS (1983) J Am Ceram Soc 66:18
10. Hund F (1985) Z Anorg Allg Chem 525:221
11. Mchale AE, Roth RS (1986) J Am Ceram Soc 69:827
12. Wilson G, Glasser FP (1989) Br Ceram Trans J 88:69
13. Yoshikawa Y, Tsuzuki K (1990) J Am Ceram Soc 73:31
14. Parker FJ (1990) J Am Ceram Soc 73:929
15. Hirano S, Hayashi T, Hattori A (1991) J Am Ceram Soc 74:1320
16. Azough F, Wright A, Freer R (1994) J Solid State Chem 108:284
17. Colon G, Aviles MA, Navio JA, Sanchez-Soto PJ (2002) J Therm Anal Cal 67:229
18. Wang I, Chang WF, Shiau RJ, Wu JC, Chung CS (1983) J Catal 83:428
19. Daly FP, Ando H, Schmitt JL, Sturm EA (1987) J Catal 108:401
20. Huang P-N, Secco EA (1993) J Solid State Chem 103:314
21. Lee J-H, Yoon SM, Kim B-K, Lee H-W, Song HS (2002) J Mater Sci 37:1165, DOI: 10.1023/A:1014363304942
22. Shashi K, Wagner JB Jr (1980) J Appl Phys Lett 37:757
23. Idem (1981) J Phy Rev B 23:6417
24. Idem (1982) J Phy Chem Solids 43:713
25. Samsonov GV (1982) The oxide handbook, IFI/PLENUM, New York
26. Rao CNR, Rao KJ (1978) Phase transitions in solids. McGraw-Hill, New York, p 263
27. Nair SM, Yahya AI, Afaq Ahmad (1996) J Solid State Chem 122:349
28. Kumari MS, Secco EA (1978) Can J Chem 56:2616
29. Kumari MS, Secco EA (1985) Can J Chem 63:324
30. Sohn JR, Kim J-G, Kwon T-D, Park EH (2002) Langmuir 18(5):1666
31. Bondioli F, Leonelli C, Manfredini T (2005) J Am Ceram Soc 88:633
32. Turkoglu O, Belenli I (2003) J Therm Anal Cal 73:1001
33. Kahlert H, Frey F, Boysen H, Lassak K (1995) J Appl Cryst 28:812
34. Teixeira V, Andristschky M, Fischer W, Buchkremer HP, Stoever D (1999) Surf Coat Technol 120–121:103
35. Levin EM, Mcmurdie NF (1975) In: Reser MK (ed) Phase diagrams for ceramics, The American Ceramic Society, Columbus, OH, p. 76
36. Adamski A, Sojka Z, Dyrek K, Che M (1999) Solid State Ionics 117:113